Appl. Phys. B (2004)
DOI: 10.1007/s00340-004-1639-7

Applied Physics B
Lasers and Optics

D. WEIDMANN[1,*,✉]
G. WYSOCKI[1]
C. OPPENHEIMER[2]
F.K. TITTEL[1]

Development of a compact quantum cascade laser spectrometer for field measurements of CO_2 isotopes

[1] Rice Quantum Institute, Rice University, 6100 Main Street, Houston, TX, USA
[2] Department of Geography, Downing Place, Cambridge CB2 3EN, UK

Received: 10 August 2004
Published online: 29 September 2004 •

ABSTRACT We report the development of a field-deployable, pulsed quantum cascade laser spectrometer. The instrument is designed to measure the $^{13}C/^{12}C$ isotopic ratio in the CO_2 released from volcanic vents. Specific $^{12}CO_2$ and $^{13}CO_2$ absorption lines were selected around 4.3 μm, where the P-branch of $^{12}CO_2$ overlaps the R-branch of $^{13}CO_2$ of the 00^01–00^00 vibrational transition. This particular selection makes the instrument insensitive to temperature variations. A dual-channel cell balances the two absorption signals. We provide details of the instrument design and a preliminary demonstration of its performance based on laboratory measurements of $^{16}O^{12}C^{16}O$ and $^{16}O^{12}C^{18}O$.

PACS 42.55.Px; 42.62.Fi; 07.88.+y

1 Introduction

Measurements of stable isotopic ratios of carbon (in addition to other species including hydrogen, nitrogen, oxygen and sulfur) provide unique information about the source and history of the compound under study through an understanding of fractionation and mixing processes. Isotopic ratiometry has important applications in many fields, including atmospheric sciences, biochemistry and geochemistry. For atmospheric chemistry and environmental monitoring the main purpose of carbon isotopic measurements is to determine carbon sources and sinks (see [1] and references therein). In biochemistry, concentrations of carbon isotopes are relevant to studies of photosynthesis, and have applications for non-invasive, early diagnostics by breath analysis [2]. Geochemical applications are varied [3] and include evaluation of the sources of volcanic gases, critical to eruption forecasting and volcanic hazard assessment. For example, the ratio $^3He/^4He$ is useful in distinguishing magmatic helium from that derived radiogenically in the Earth's crust (and enriched in ^4He) [4]. It has been shown recently that this ratio can be measured by near-infrared laser spectroscopy [5]. Nitrogen isotopic composition traces sedimentary input into volcanic gases [6], while concentrations of ^{18}O and D in water composition are important indicators of mixing of magmatic, hydrothermal, marine and meteoric sources. Stable isotopes of carbon and sulfur can reveal magma sources, assuming that isotopic compositions of surface reservoirs are constrained. For example, $^{13}CO_2/^{12}CO_2$ and $^{34}SO_2/^{32}SO_2$ measurements of gas samples collected from the lava lake of Erta 'Ale volcano (Ethiopia) indicated the mantle origin of emitted carbon and sulfur ($\delta^{13}C \approx -4‰$ and $\delta^{34}S \approx 0‰$), whereas emissions from 'arc' volcanoes display more variable $\delta^{13}C$ (-12 to $+2.5‰$) and $\delta^{34}S$ (0 to $+10‰$) due to contamination by sedimentary and crustal sources [7].

Isotopic ratios are commonly expressed as 'delta values'. For the $^{12}C/^{13}C$ ratio in CO_2 the $\delta^{13}C$ value is defined as follows:

$$\delta^{13}C = \frac{R_X - R_{PDB}}{R_{PDB}} \times 1000\,. \quad (1)$$

Note that this notation means that delta values are expressed as 'per mil' (parts per thousand, or ‰). R denotes the concentration ratio of $^{13}CO_2$ and $^{12}CO_2$. R_X refers to the sample to be analyzed and R_{PDB} to the Vienna Pee Dee Belemnite standard ($R_{PDB} = 0.0112312$ [8, 9]). The value of R_{PDB} is high (high ^{13}C) relative to a number of environmental sources and therefore $\delta^{13}C$ is typically negative. For example, the average value in the atmosphere is $\sim -8‰$.

Isotope ratio mass spectrometry (IRMS) is the standard measurement technique, and has been used successfully for many years, with a precision in the 0.01‰–0.05‰ range. However, IRMS cannot differentiate isotopes with almost the same mass, it does not allow real-time measurements, it often requires a complex sample preparation and precision IRMS instrumentation is not readily field deployable for in situ measurements. To overcome these issues, when a target precision of $\sim 0.1‰$ is required, techniques based on infrared absorption spectroscopy offer an alternative approach. An excellent up-to-date review of these techniques can be found in [10]. In particular, tunable laser absorption spectroscopy based on semiconductor lasers promises compact instrumentation and real-time measurements. These sensors can discriminate closely related lines of different isotopes due to their narrow instrumental bandwidths.

We report here the development of a field-deployable instrument designed for measurement of volcanic emissions, and based on tunable infrared laser absorption spectroscopy.

✉ Fax: +1-713-348-5686, E-mail: d.weidmann@rl.ac.uk
Present address: Space Science and Technology Department, CCLRC Rutherford Appleton Laboratory, Chilton, Didcot, Oxfordshire, OX11 0QX, UK

The spectroscopic source used is a distributed feedback (DFB) quantum cascade laser (QCL) operating at Peltier-cooled temperatures in a pulsed mode and emitting at 4.3 μm. This mid-infrared source is well suited for a field-deployable instrument because it does not require liquid-nitrogen cooling, it is compact and robust, provides several mW of power and can access a fundamental band of CO_2.

First, we discuss the choice of the $^{12}CO_2$ and $^{13}CO_2$ lines to be used, and review prior work on $^{13}CO_2/^{12}CO_2$ ratio measurements by semiconductor laser absorption spectroscopy. We then describe in detail the instrument design and report a laboratory demonstration of the instrument capabilities.

2 $^{13}CO_2$ and $^{12}CO_2$ line selection

Prior to selection of the optimum CO_2 absorption lines, the general spectral region for measurement is determined primarily by the available laser source, in this case a QCL. Figure 1 presents the $^{12}CO_2$ and $^{13}CO_2$ bands in the near and mid infrared, obtained from the HITRAN 2000 database [11]. The most favorable band to measure $\delta^{13}C$ with high precision appears to be the ν_3 band centered at 2349 cm^{-1} (4.3 μm). Also, the ν_2 band centered at 667 cm^{-1} (15.0 μm) and the combination band $\nu_1 + \nu_3$ centered at 3720 cm^{-1} (2.7 μm) could be used, but their intensities are a factor of about one hundred weaker than the ν_3 band.

Although far from optimum in terms of transition intensity, the $^{13}C/^{12}C$ isotope ratio has been measured using a harmonic band in the near-infrared region. The availability of near-infrared semiconductor lasers, their low cost and reliability and the possibility of fiber amplification and coupling make this spectral region very attractive. For example, Gagliardi et al. and Rocco et al. measured $^{13}CO_2/^{12}CO_2$ at ~ 2 μm (5000 cm^{-1}) and partially compensated the intrinsic low line strength (of more than three orders of magnitude weaker than the ν_3 band) by using a multipass cell [12, 13]. Measurements have also been performed with telecommunications laser diodes at 1.6 μm (6250 cm^{-1}), where lines are about five orders of magnitude weaker than in the ν_3 band [14, 15]. At these wavelengths, the weak absorption lines can be compensated by use of highly sensitive cavity ring-down spectroscopy [2].

Having found a suitable absorption band, the precise $^{12}CO_2$ and $^{13}CO_2$ transitions have to be selected. Two main

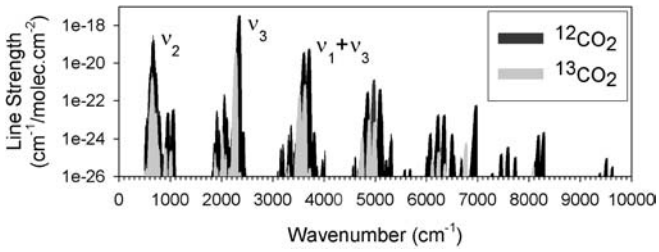

FIGURE 1 Ro-vibrational bands suitable for $^{12}CO_2/^{13}CO_2$ ratio measurements, based on HITRAN 2000

criteria dictate this choice. Firstly, the signals for each isotope should be of similar intensities in order to limit the effect of the intrinsic non-linearity due to Beer's law and potential non-linearities of the detectors. In practice, this means that the overall absorption of the $^{12}CO_2$ and the $^{13}CO_2$ lines must be similar. Secondly, the lower energy levels of the $^{12}CO_2$ and $^{13}CO_2$ transitions must be as close as possible to limit the sensitivity of the measurement to temperature variations. This dependence is approximately given by [16]

$$\Delta T\, \Delta E = \Delta\delta\, kT^2\,, \tag{2}$$

where ΔT is the temperature variation, ΔE the difference between the lower-state energies of the $^{12}CO_2$ and $^{13}CO_2$ transitions, $\Delta\delta$ the corresponding precision of the delta value, k the Boltzmann constant and T the temperature. These criteria cannot be fulfilled together in the 2300 cm^{-1} region. In addition, the lines have to be the strongest possible to achieve good sensitivity, the spectral window must be free of atmospheric interference and the two line frequencies close enough to resolve with a single QCL scan.

From these considerations, two strategies are feasible. Either two lines can be selected such that the strengths of the $^{12}CO_2$ and $^{13}CO_2$ absorptions are similar. In this case, the transition lower-state energies are quite different and the temperature of the gas mixture during measurements has to be very stable. Alternatively, two lines with almost the same lower-state energy can be selected. In this case, the line intensities are different and the respective absorptions have to be balanced using a dual-channel absorption cell [1, 17].

Several techniques with different line-selection strategies have already been developed to measure the $^{13}CO_2/^{12}CO_2$ ratio using the ν_3 band. An analyzer based on difference-

	Technology	Line selection for ^{12}C and ^{13}C (cm^{-1})	Line intensity ratio 12/13	ΔT (K)	$\Delta\delta$ (‰)
Erdelyi et al. [18]	DFG	2299.642357 2299.795519	0.67	0.005	0.8
Mc Mannus et al. [1]	Lead salt Dual path	2314.304896 2314.408412	46	0.213	0.2
Becker et al. [20]	Lead salt	2291.541690 2291.680391	0.64	0.004	4
Bowling et al. [19]	Lead salt	2308.224689 2308.171080	0.43	0.006	0.25
This work	QCL Dual path	2311.105566 2311.398738	96	181	

TABLE 1 Summary of tunable mid-infrared laser-based spectroscopy approaches for $^{12}CO_2/^{13}CO_2$ isotopic ratio measurements. The frequencies and intensity ratios of the two transitions chosen in each case are given. ΔT is the corresponding temperature stability required to achieve a 0.1‰ precision in $\delta^{13}C$. The last column indicates the precision achieved

frequency generation was reported by Erdélyi et al. with a 0.8‰ precision [18]. Lead salt diode laser spectrometers have also been used, delivering precisions of 0.2‰ [1], 0.25‰ [19] and 4‰ [20, 21]. An instrument based on a pulsed QCL is also in development at Physical Science Inc. [22]. The line selections for these different studies are compared in Table 1.

We selected a line pair around 2311 cm^{-1}. The main feature is that the two transitions have nearly the same lower-state energies. The calculated required temperature stability to achieve a 0.1‰ precision on the delta value is 180 K, which means that CO_2 isotopic ratio measurement will be insensitive to temperature fluctuations. On the other hand, the two line strengths are very different (the ratio is 96) and can be compensated for using different path lengths for each line.

3 Description of dual gas absorption cells

The selected $^{12}CO_2$ line has a high intensity of $\sim 10^{-19}$ cm^{-1}/molec. cm^{-2}. As the CO_2 concentration is expected to be greater than 1% in volcanic gas emissions, a short path length is needed to avoid saturation. We have constructed an optical configuration consisting of two separate cells, by modifying a 36-m multipass astigmatic Herriott cell from Aerodyne Research Inc. [23]. The cell entrance window has been replaced by a short-path cell (Fig. 2), whose exit window acts as a beam splitter coupling a part of the laser radiation into the Herriott cell. The two windows are parallel to ensure that the path length does not depend on the beam position.

The incoming beam from the QCL follows two separate optical paths:

- Channel 1, short path ($^{12}CO_2$): the beam enters the short-path cell via the entrance window (CaF_2 wedge), transits through the short-path cell (0.024 m) and exits via a wedged ZnSe window.
- Channel 2, long path ($^{13}CO_2$): the beam enters the short-path cell as for channel 1. The beam is then reflected by the ZnSe window and travels in the astigmatic Herriott cell. The beam makes 12 passes inside the multipass cell (2.444 m) and then exits through the ZnSe window.

Channels 1 and 2 transmit 44% and 12% of the incoming QCL power, respectively. The two cells are interconnected so that the gas to be measured is at the same pressure in each channel. Figure 3 shows simulated spectra for these conditions and a concentration of 1% CO_2 in air at 50 Torr for the natural abundance of $^{13}CO_2$.

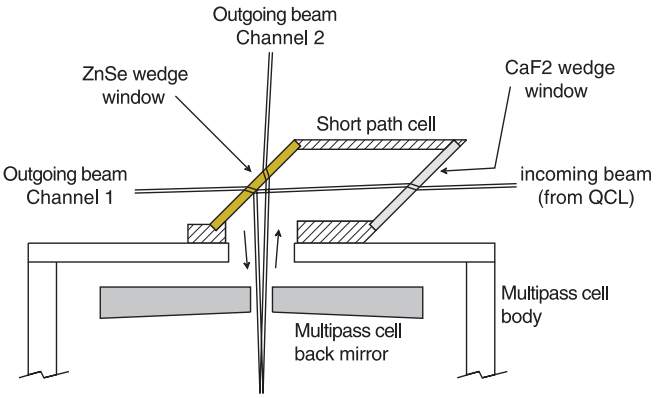

FIGURE 2 Schematics of the modified Herriott cell. Note the two different path lengths

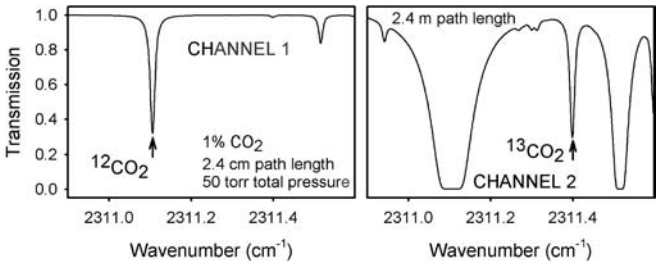

FIGURE 3 Simulated spectra for the two cells (channels 1 and 2) for a total pressure of 50 Torr, a CO_2 concentration of 1% and the natural isotopic abundance. The lines of interest are indicated by an *arrow*

4 CO_2-sensor design

4.1 *Optical platform*

The two absorption cells, the QCL source, detectors and other components are mounted on a 46×30 cm^2 optical breadboard. A plan view and a three-dimensional (3D) view of the optical platform are shown in Figs. 4 and 5, re-

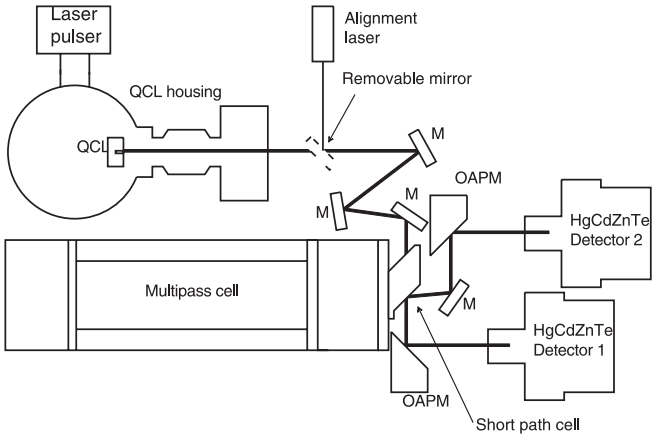

FIGURE 4 Scaled optical layout of the sensor. M indicates plane mirrors, and OAPM off-axis parabolic mirrors

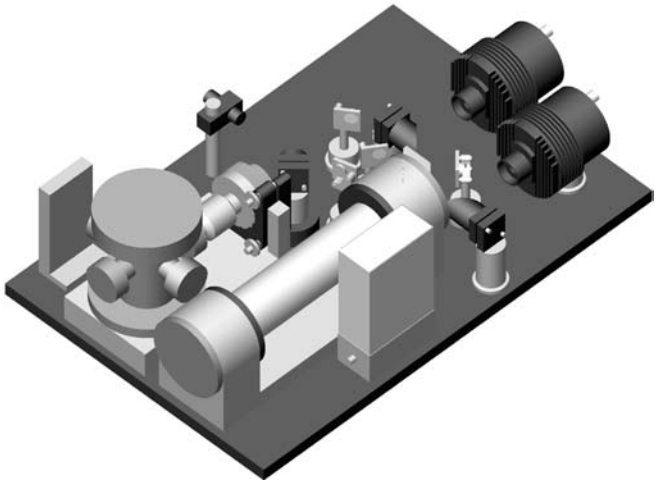

FIGURE 5 3D view of the optical head of the sensor on the 46×30 cm^2 optical breadboard

spectively. The QCL is enclosed in an evacuated housing [24]. The exiting infrared beam is collimated with a ∼ 6-mm diameter, f/0.5 aspheric ZnSe lens. High-current ns pulses are provided by a laser driver (Directed Energy model PCO-7120) to the QCL via a low-impedance strip line. After the exit window of the QCL housing, a removable mirror can be inserted for beam alignment. This mirror redirects the beam coming from a visible diode laser and allows the superimposition of the visible and mid-infrared beams. Except during the alignment process, the QCL beam encounters a set of three mirrors, which are used to couple the QCL beam to the dual-cell system. As shown in Fig. 2, two beams exit the absorption cell system and are focused on two detectors by 75 mm focal length off-axis parabolic mirrors. Two thermoelectrically cooled photovoltaic HgCdZnTe detectors (VIGO Systems model PDI-2TE-5) are used. The effective area of each detector is 1 mm^2 and their response time is ∼ 20 ns. The detectors are connected to transimpedance preamplifiers with a 50-MHz bandwidth, and their outputs are sent to the data-acquisition system. The optical module of the sensor is sealed off and a constant low overpressure of dry nitrogen is applied to prevent contamination of the sensor by ambient atmospheric CO_2.

4.2 *Data acquisition*

The peak voltage of the detected optical pulses is measured using 350-MHz sampling bandwidth track and hold (T&H) circuits [25]. Data acquisition is performed by a National Instrument PCMCIA card (DAQ card Al-16E-4) connected to a laptop computer. Software control was implemented using LabView.

External timing was used to optimize the acquisition rate (see Fig. 6). Four acquisition channels were used: two for the QCL peak signal (laser on), and two for the detector background voltage (laser off). The reference clock operates at 50 kHz and synchronizes the laser excitation signal. This excitation signal consists of a 20-ns-width pulse sent to the gate input of the laser driver, which delivers a 25-ns current pulse train to the QCL. At the same time, this signal clocks the scan sequence of the acquisition card. The gate signals provided to the two T&Hs run at twice the reference frequency so that two sequences can be recorded: one with the laser on, the other with the laser off (background). For each gate, the delay and length of the holding time have to be adjusted: the delay is set such that the T&H gate signal rising edge corresponds to the position of the detected pulse peak voltage, and the 'holding time' must be sufficiently long in order to keep the captured voltage to be acquired by the DAQ card. These parameters must be optimized for the two channels of the spectrometer. The acquisition clock runs at four times the reference frequency (four channels must be acquired) with its delay time adjusted so that acquisition sequences appear within the holding time of both T&Hs. The user can select the number of spectra that are required for averaging.

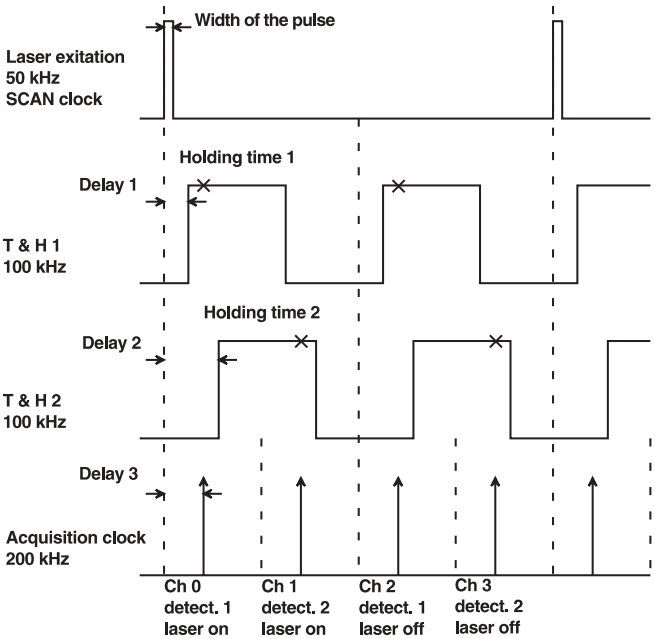

FIGURE 6 Timing diagram of the acquisition sequence. The *crosses* indicate individual acquisitions

4.3 *Gas-flow system*

The gas-flow system uses a compact diaphragm pump, a pressure controller and four three-way electromagnetic valves driven by the digital output of the data-acquisition card. The gas input can be switched between dry nitrogen, an isotopic calibration mixture (the reference gas) and the sample. Isotopic calibration standards are costly and we therefore use a separate holding tank in order to recycle the reference gas in a closed loop, as noted previously [18].

The complete architecture of the control system is summarized in Fig. 7, and a photograph of the actual sensor is depicted in Fig. 8.

5 Measurement protocol

Measurements are performed as follows:

– Acquisition of spectra for a calibrated isotopic gas mixture. We use a calibrated reference cylinder from Cambridge Isotope Laboratories Inc. (with its $\delta^{13}C$ value, δ_{cal}, known with a precision of 0.01‰) for the determination of $[^{12}C_{cal}]$ and $[^{13}C_{cal}]$.

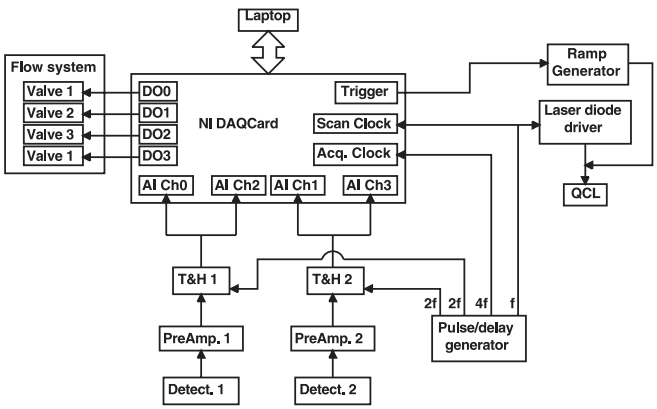

FIGURE 7 Scheme of the electronic control and data-acquisition system of the laser-based gas sensor. DO, digital output; AI Ch, analog input channel

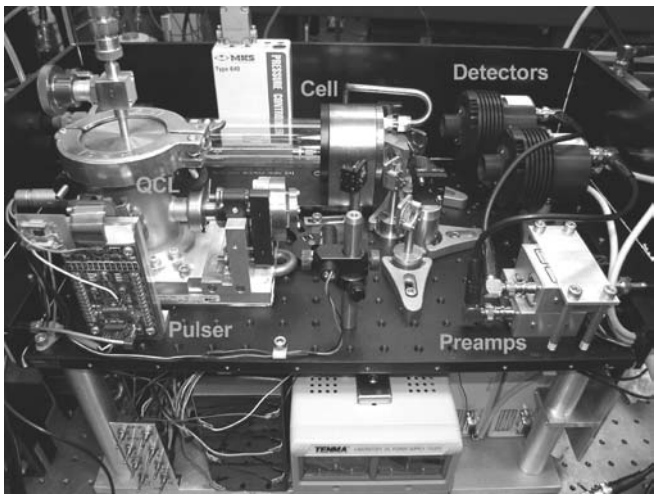

FIGURE 8 Spectrometer shown with the cover removed. Power supplies and controllers are housed below the main optical breadboard

- Acquisition of spectra for the unknown sample for which $[^{12}C_X]$ and $[^{13}C_X]$ are to be determined.
- A baseline can be recorded by purging the system with dry nitrogen, if required.

The unknown δ_X is then given by

$$\delta_X = \delta_{\text{cal}} + \frac{R_X - R_{\text{cal}}}{R_{\text{PDB}}} \times 1000\,. \tag{3}$$

6 Instrumental sensitivity

Retrieval of concentrations is made by line integration of the absorbance signal $\alpha(\nu)$. In this case, the concentration is given by

$$C = \frac{\int \alpha(\nu)\,\mathrm{d}\nu\; RT}{L\,S\,N_{\text{A}}\,P}\,, \tag{4}$$

where R is the ideal gas constant, T the temperature, L the path length, S the line intensity, N_{A} Avogadro's number and P the pressure. By differentiating (3), we obtain the precision of the delta value as a function of the precision of the concentration measurement:

$$\Delta\delta_X \approx \frac{2000\,\Delta C}{R_{\text{PDB}}\;[\text{CO}_2]}\,, \tag{5}$$

where the concentration precision ΔC is assumed to be identical for the measurements of $[^{13}CO_2]$ and $[^{12}CO_2]$ in both channels, and $[^{13}CO_2] \ll [^{12}CO_2]$. From (5), it can be shown that, for a 1% CO_2 mixture, a precision of 10 ppb in the concentrations is required to achieve a 0.2‰ precision in $\delta^{13}C$. This means that the pressure stability inside the optical cells must be better than 0.05 mTorr, and the optical path length stability better than 2 μm.

The main sensitivity limitation is expected to arise from the usual performance issues of pulsed QCL-based spectrometers [26]: an increase in laser line width as a result of thermal chirping and pulse-to-pulse intensity variations. Hence, achieving a 0.1‰ precision in $\delta^{13}C$ is a significant technical challenge to implement.

7 Results of laboratory tests of the QCL-based CO_2-gas sensor

For laboratory testing of the CO_2 sensor we utilized a QCL-based spectroscopic source operating at 2320 cm^{-1}, as it was the only commercially available QCL for this spectral region at this time. However, it operated outside the 2311-cm^{-1} spectral region identified to be optimum for $^{13}CO_2$ isotopic measurements as described in Sect. 2. This QCL was nevertheless valuable for demonstrating the basic concept of the sensor by examining the $^{16}O^{12}C^{18}O$ isotope concentration. The specifications of this particular QCL were unusual as compared to other QCLs. For example, a threshold peak current of about 8 A at −35 °C when compared to less than 1 A for a usual QCL. Such a high injection current results in two major issues:

- The thermal chirp, and consequently the laser line width, was broadened.
- The optical frequency was limited in tunability when applying a subthreshold current ramp because of the high thermal load of the QCL.

Hence, laser-frequency scanning was performed by temperature tuning. The peak current of the excitation pulse was set to 8.2 A, which is close to the laser threshold. A 7 °C temperature ramp from −28 to −35 °C was applied. Each acquisition point lasted 8 ms and consisted of 400 co-added (averaged) acquisition events. For these tests a flow of a calibrated mixture of CO_2 diluted (1.00 ± 0.02%) in dry nitrogen was used. The pressure in the absorption cell was set to 50 Torr. The tuning rate was measured to be $-0.12\,\text{cm}^{-1}\,\text{K}^{-1}$ and the averaged QCL power was 0.2 mW.

The spectra recorded simultaneously by the two channels are shown in Fig. 9.

Figure 9a shows the signal from the short-path cell. Only the intense $^{12}CO_2$ lines are visible. In this plot is also depicted the theoretical transmission expected according to HITRAN

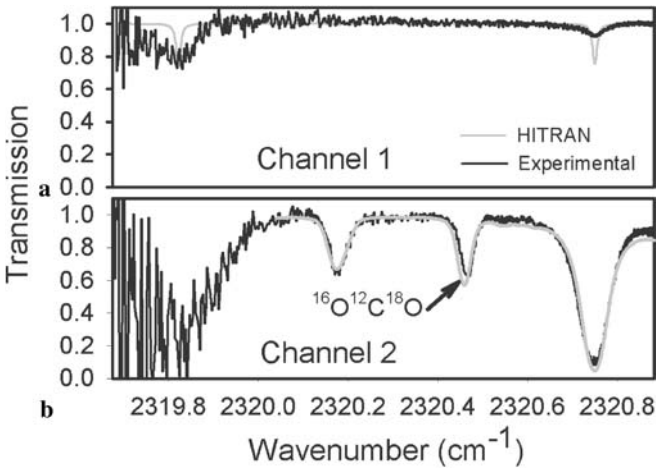

FIGURE 9 Spectra for $^{16}O^{12}C^{18}O$ recorded to demonstrate the basic concept of the instrument. (**a**) corresponds to the short path cell signal; (**b**) is the signal from the long path. The simulated spectra from HITRAN are shown in *light grey*. In (**a**) the laser line width has not been taken into account, whereas in (**b**) a 0.04 cm^{-1} FWHM Gaussian function simulated the laser line width

(grey trace). The comparison between the experimental and the theoretical spectra points out the effect of the laser spectral width. The 1σ noise on either side of the $^{16}O^{12}C^{16}O$ line at $2320.75\,cm^{-1}$ is 1.2×10^{-2}. By computing the area below the absorbance curve and using (4), the retrieved concentration for $^{16}O^{12}C^{16}O$ is $1.00\pm0.06\%$. The line parameters from HITRAN were used. For these particular lines, the quoted precision in the intensities is given as 5% and therefore represents the major source of uncertainty in the concentration retrieval.

In the second channel (see Fig. 9b), the intense $^{16}O^{12}C^{16}O_2$ line nearly saturates and a $^{16}O^{12}C^{18}O$ line appears (indicated by an arrow). In Fig. 9b is also depicted the HITRAN calculated spectrum but this time convolved with a $0.04\,cm^{-1}$ FWHM Gaussian function. The agreement is very good, as can be seen. We believe that discrepancies can be further reduced by refining the function that describes the laser emission spectrum known as not being purely Gaussian. For the calculated spectrum the natural abundance of $^{16}O^{12}C^{18}O$ has been used in the calculation (0.394707%) and the isotopic line at $2320.46\,cm^{-1}$ is in good agreement with the experimental one. At longer wavelengths an increase in noise is apparent. This is due to laser intensity variation during temperature tuning.

8 Conclusions

We have reported the development of a field-deployable QCL-based sensor for measurements of CO_2 isotopes. The sensor consists of a dual absorption cell and is based on the selection of a particular pair of absorption lines that yield ^{13}C and ^{12}C concentration measurements that are insensitive to temperature. We have demonstrated the basic sensor concept by measuring $^{16}O^{12}C^{16}O$ and $^{16}O^{12}C^{18}O$ concentrations in a 1% CO_2 mixture in N_2 in the spectral region of $2320\,cm^{-1}$. In future, a dedicated pulsed QCL that emits at $2311\,cm^{-1}$ will be integrated into the instrument to investigate the experimental precision achievable in $\delta^{13}C$, prior to full field testing. Several groups have reported progress in the development of thermo-electrically cooled continuous-wave QCLs [27–29] and interband cascade lasers [30] as well as advanced compact DFG-based sources [31], which would further improve the performance of the reported CO_2 spectrometer.

ACKNOWLEDGEMENTS The authors are grateful to K. Uehara of Keio University for helpful discussions and input to this work. The authors also gratefully acknowledge financial support from the National Aeronautics and Space Administration, the Texas Advanced Technology Program, the Robert Welch Foundation and the Office of Naval Research via a sub-award from Texas A&M University as well as from the Gruppo Nazionale per la Vulcanologia and Istituto Nazionale di Geofisica e Vulcanologia (under a grant entitled 'Development of an integrated spectroscopic system for remote and continuous monitoring of volcanic gas'). C. Oppenheimer was additionally supported by the UK Natural Environment Research Council (by Grant No. GR9/04655 entitled 'Field measurement of volcanic gas concentration ratios and isotopes by laser spectroscopy').

REFERENCES

1 J.B. McManus, M.S. Zhaniser, D.D. Nelson, L.R. Williams, C.E. Kolb: Spectrochim. Acta Part A **58**, 2565 (2002)
2 E.R. Crosson, K.N. Ricci, B.A. Richman, F.C. Chilese, T.G. Owano, R.A. Provencal, M.W. Todd, J. Glasser, A.A. Kachanov, B.A. Paldus, T.G. Spence, R.N. Zare: Anal. Chem. **74**, 2003 (2002)
3 J.W. Valley, D. Cole (Eds.): *Stable Isotope Geochemistry* (Rev. Mineral.) (Mineralogical Society of America, Washington, DC 2001)
4 M.L. Sorey, W.C. Evans, B.M. Kennedy, C.D. Farrar, L.J. Hainsworth, B. Hausback: J. Geophys. Res. **103**, 303 (1998)
5 L.B. Wang, P. Mueller, R.J. Holt, Z.T. Lu, T.P. O'Connor, Y. Sano, N.C. Sturchio: Geophys. Res. Lett. **30**, 1592 (2003)
6 T.P. Fischer, D.R. Hilton, M.M. Zimmer, A.M. Shaw, Z.D. Sharp, J.A. Walker: Science **297**, 1154 (2002)
7 P. Delmelle, J. Stix: 'Volcanic Gases'. In: H. Sigurdsson, B.F. Houghton, S.R. McNutt, H. Rymer, J. Stix (eds.): *Encyclopedia of Volcanoes* (Academic, San Diego, California, USA 2000) p. 803
8 H. Graig: Geochim. Cosmochim. Acta **12**, 133 (1957)
9 C.E. Allison, R.J. Francey, H.A.J. Meijer: IAEA-TECDOC-825, 155 (1995)
10 E. Kerstel: in *Handbook of Stable Isotope Analytical Techniques*, ed. by P.A. de Groot (Elsevier, to be published 2004)
11 L.S. Rothman, A. Barbe, D.C. Benner, L.R. Brown, C. Camy-Peyret, M.R. Carleer, K. Chance, C. Clerbaux, V. Dana, V.M. Devi, A. Fayt, J.-M. Flaud, R.R. Gamache, A. Goldman, D. Jacquemart, K.W. Jucks, W.J. Lafferty, J.-Y. Mandin, S.T. Massie, V. Nemtchinov, D.A. Newnham, A. Perrin, C.P. Rinsland, J. Schroeder, K.M. Smith, M.A.H. Smith, K. Tang, R.A. Toth, J. Vander Auwera, P. Varanasi, K. Yoshino: J. Quantum Spectrosc. Radiat. Transfer **82**, 5 (2003)
12 G. Gagliardi, A. Castrillo, R.Q. Iannone, E.R.T. Kerstel, L. Gianfrani: Appl. Phys. B **77**, 119 (2003)
13 A. Rocco, G. De Natale, P. De Natale, G. Gagliardi, L. Gianfrani: Appl. Phys. B **78**, 235 (2004)
14 D.E. Cooper, R.U. Martinelli, C.B. Carlisle, H. Riris, D.B. Bour, R.J. Menna: Appl. Opt. **32**, 6727 (1993)
15 R. Chaux, B. Lavorel: Appl. Phys. B **72**, 237 (2001)
16 P. Bergamaschi, M. Schupp, G.W. Harris: Appl. Opt. **33**, 7704 (1994)
17 K. Uehara, K. Yamamoto, T. Kikugawa, N. Yoshida: Sens. Actuators B **74**, 173 (2001)
18 M. Erdélyi, D. Richter, F.K. Tittel: Appl. Phys. B **75**, 289 (2002)
19 D.R. Bowling, S.D. Sargent, B.D. Tanner, J.R. Ehleringer: Agr. Forest Meteorol. **118**, 1 (2003)
20 J.F. Becker, T.B. Sauke, M. Loewenstein: Appl. Opt. **31**, 1921 (1992)
21 T.B. Sauke, J.F. Becker: Planet. Space Sci. **46**, 805 (1998)
22 D.M. Sonnenfroh, M.L. Silva, M.G. Allen: 'A Quantum Cascade Laser-based Sensor for Measurement of the Stable Isotopomers of Carbon Dioxide'. In: *Laser Applications to Chemical and Environmental Analysis (LACEA), Annapolis, MD, 11 February 2004*, paper WA4
23 J.B. McManus, P.L. Kebabian, M.S. Zahniser: Appl. Opt. **34**, 3336 (1995)
24 A.A. Kosterev, R.F. Curl, F.K. Tittel, R. Köhler, C. Gmachl, F. Capasso, D.L. Sivco, A.Y. Cho: Appl. Opt. **41**, 573 (2002)
25 G. Wysocki, M. McCurdy, S. So, D. Weidmann, C. Roller, R.F. Curl, F.K. Tittel: Appl. Opt. **42** (2004)
26 D.D. Nelson, J.H. Shorter, J.B. McManus, M.S. Zahniser: Appl. Phys. B **75**, 343 (2002)
27 T. Aellen, S. Blaser, M. Beck, D. Hofstetter, J. Faist, E. Gini: Appl. Phys. Lett. **83**, 1929 (2003)
28 S. Blaser, L. Hvozdara, Y. Bonetti, A. Muller, M. Giovannini, J. Faist: in *CLEO 2004, San Francisco, CA, 16–21 May 2004*, postdeadline paper CPDB6
29 A. Evans, J.S. Yu, J. David, L. Doris, K. Mi, S. Slivken, M. Razeghi: Appl. Phys. Lett. **84**, 314 (2004)
30 R.Q. Yang, C.J. Hill, B.H. Yang, C.M. Wong, R.E. Muller, P.M. Echternach: Appl. Phys. Lett. **84**, 3699 (2004)
31 D. Richter, A. Fried, B.P. Wert, J.G. Walega, F.K. Tittel: Appl. Phys. B **75**, 281 (2002)